American Mineralogist, Volume 93, pages 124–133, 2008

Crystal-size distribution and composition of garnets in eclogites from the Dabie orogen, central China

Hao Cheng,[1,2,*] Zuyi Zhou,[1] and Eizo Nakamura[2]

[1]State Key Laboratory of Marine Geology, Tongji University, Shanghai 200092, P.R.China
[2]The Pheasant Memorial Laboratory for Geochemistry and Cosmochemistry, Institute for Study of the Earth's Interior, Okayama University at Misasa, Tottori 682-0193, Japan

Abstract

Crystal-size and spatial distributions of minerals in metamorphic rocks provide insight into their nucleation, growth environment, and the metamorphic evolution of their host rocks. Episodic nucleation and growth histories for garnets in eclogites from the Dabie orogen are revealed by variations in crystal size, geochemical zoning, and mineralogy of inclusions in garnets. The studied garnets show pseudo-lognormal crystal-size distributions (CSDs), prograde chemical zoning patterns indexed by mineral inclusions, and are mainly distributed at random. Constant growth rate for each episode is proposed based on the mineralogy of inclusions in garnets and the chemical zoning patterns. The CSD shapes were evaluated in terms of a size-dependent proportionate growth model and a thermally accelerated, diffusion-controlled model but neither is consistent with the geochemical data and the concordant occurrence of mineral inclusions in garnet. Initial increasing nucleation rate followed by a subsequent, medial stage of nearly constant growth and finally declining nucleation rate is inferred from the CSD data. This study suggests that linking chemical analysis with textural analysis is crucial to avoid misleading interpretation solely through CSD shapes of minerals in metamorphic rocks.

Keywords: Garnet, crystal size, zoning, growth, Dabie

Introduction

Insights into the nucleation and growth of crystals during metamorphism are essential to understand metamorphic processes and can be gained from quantitative textural and chemical analyses. Garnets are a crucial record of nucleation, because they commonly preserve a record of chemical and textural variation over a wide range of metamorphic grades that can be readily simplified and interpreted due to their isotropic crystal structure. The increasing numbers of CSD studies of garnets in various rocks have improved our understanding of their nucleation and growth environment (e.g., Kretz 1993; Carlson 1999). Several types of CSDs have been documented in various natural rock studies; however, the controlling factors of the CSD evolution are still debated. Several interpretations of garnet nucleation and crystallization mechanisms have been invoked, for example: (1) constant nucleation and growth rate with subsequent (Ostwald ripening) coarsening (Cashman and Ferry 1988; Miyazaki 1991); (2) thermally accelerated, diffusion-controlled nucleation and growth (Carlson 1999; Denison and Carlson 1997); (3) continuous nucleation and linear rate of growth (Kretz 1993, 2006); and (4) size-dependent crystal growth (Eberl et al. 1998).

Since being introduced to geology (Marsh 1988), CSD analyses have been implemented primarily in igneous rock studies (e.g., Cashman and Marsh 1988; Peterson 1990; Armienti et al. 1994; Higgins 1996, 1998, 2002; Wilhelm and Wörner 1996; Armienti and Tarquini 2002; Martin et al. 2006; Browne et al. 2006; Kinman and Neal 2006). In contrast, few CSD analyses have focused upon metamorphic rocks (Cashman and Ferry 1988; Carlson 1999; Kaneko et al. 2005; Kretz 2006), and ultrahigh-pressure (UHP) metamorphic rocks remain unexplored. Moreover, CSD analysis of the subduction-related UHP metamorphic rocks not only can shed light on the garnet nucleation and growth mechanism but also should yield additional insights into subduction and exhumation processes as garnets respond to the prograde and retrograde metamorphic evolution of their host rocks.

In this study, we examined the size and spatial distribution of garnets in eclogites from the Dabie UHP metamorphic belt in central China by applying a serial grinding strategy, together with garnet chemical analyses by electron microprobe to evaluate the capability of CSD analyses to explore nucleation and growth mechanisms of metamorphic minerals. Our results highlight the importance of linking chemical and textural analysis when interpreting the CSDs of minerals in metamorphic rocks.

Sample description

The eclogites investigated here are located at Taihu in southern Dabie, central China, an extensive ultrahigh-pressure metamorphic belt that is generally considered as the suture zone formed by the collision of the Yangtze and Sino-Korean cratons during the Triassic (e.g., Ames et al. 1993; Eide et al. 1994; Rowley et al. 1997; Hacker et al. 1998; Li et al. 2000). Detailed geologic and petrologic descriptions of the studied eclogites can be found elsewhere (Wang and Liou 1991; Okay

* E-mail: chenghao@mail.tongji.edu.cn

1993; Carswell et al. 1997; Castelli et al. 1998; Li et al. 2004; Shi and Wang 2006). Samples were collected from two outcrops at Taihu, namely TH09 and TH12; their mineral assemblages consist of garnet, omphacite, quartz, clinozoisite, paragonite, minor kyanite, retrograde amphibole, and accessory minerals including rutile and apatite. Garnet is coarse-grained and ranges up to ~2 mm in diameter, mostly having an euhedral shape with inclusions of clinozoisite, amphibole, quartz, omphacite, rutile, and apatite. Garnets are rimmed by a narrow retrograde corona of sodic amphibole preserving a hexagonal cross section (Fig. 1). The peak of eclogite-facies metamorphism, estimated at 640–670 °C and 2.4–3.3 GPa, was followed by rapid amphibolite-facies retrogression (Li et al. 2004; Shi and Wang 2006).

METHODS

Chemical analysis

Chemical compositions of garnets[1] were obtained at the Institute for Study of the Earth's Interior, Okayama University at Misasa, Japan, using a JEOL 8800 electron microprobe. Operating conditions were 15 kV accelerating voltage, 12 nA current, and counting times of 50 s on peak and 20 s each on two background measurements. Homogenous synthetic oxides and well-characterized natural garnets were used as standards. Standard ZAF correction procedures were utilized for data reduction. Sections that pass approximately through the centers of garnet crystals were obtained using the same serial grinding strategy described below for CSD analysis, but modified by applying finer grinding steps at the State Key Laboratory of Marine Geology, Tongji University. The deviation from true garnet centers is estimated to be less than 50 μm, which is the maximum grinding width (~46 μm).

Crystal-size and spatial distribution analyses

To date, most CSD data have been determined from measurements of crystal outlines in 2-D thin sections (Higgins 1994); however, the study of Mock and Jerram (2005) clearly showed that a full appreciation of the complexity and interpretative potential of the record represented by textures is best investigated using textural information obtained in three-dimensional information (Gualda and Rivers 2006). There are presently two main approaches to obtain 3-D textural information of rocks: X-ray computed tomography (e.g., Denison and Carlson 1997; Rowe et al. 1997) and serial sectioning (e.g., Bryon et al. 1995; Cooper and Hunter 1995; Mock and Jerram 2005). The size and spatial distributions of the garnets in the two eclogites from the Dabie orogen were determined by serial grinding (Kretz 2006) instead of 2-D measurement to avoid the uncertainty of data conversion from 2-D to 3-D. Because the population of crystals decreases with increasing crystal size in most rocks, uncertainty tends to increase distinctly with crystal size (Gualda and Rivers 2006). For our CSD analysis, a cubic volume rock, approximately 20 × 20 × 10 mm, was prepared using a diamond saw for serial grinding to minimize the counting statistics associated with large crystals. The grinding width was restricted below 100 μm to minimize the counting statistics error for small crystals because of the commonly observed lognormal distributions for minerals in various rocks (e.g., Eberl et al. 2002) and the increasing numbers of small crystals with increasing sample volume. Only a single volume for each sample was prepared due to the extremely heavy workload afterward. One of the volumes (TH12) was divided into four quarters to test sample homogeneity. The final five volumes were polished and immersed in a resin body and then mounted onto a slice together with three ceramic poles (Fig. 2a). The slice was then ground down gradually in 90–110 μm steps. At each step, the ground slice was mounted on an "Autoscan" high-precision 3-axis microscope stage system designed for fission track dating equipped with an external lamp-source, housed at the State Key Laboratory of Marine Geology, Tongji University. The flatness of the polished surface was verified by checking the focus of the three ceramic poles within the Z-axis. Each garnet was measured three times using the TrakScan 1.1 software and the maximum average length was regarded as the true diameter of the garnet. Tilt calibrations were made according to deviation of the last grinding surface off the horizontal surface by assuming a constant declining angle, i.e., $\theta/(n-2)$ for each grinding step (Fig. 2b). Garnets encountered in several steps could be verified by the Z-axis values and the changing trend of the measured diameters. Those that are smaller than ~100 μm can only be exposed once and the sole measured values were therefore regarded as their true sizes.

[1] Deposit item AM-08-004, data set of garnet compositions. Deposit items are available two ways: For a paper copy contact the Business Office of the Mineralogical Society of America (see inside front cover of recent issue) for price information. For an electronic copy visit the MSA web site at http://www.minsocam.org, go to the American Mineralogist Contents, find the table of contents for the specific volume/issue wanted, and then click on the deposit link there.

RESULTS

Chemical zoning

Large garnets (~1 mm) in these samples contain inclusions of clinozoisite, quartz, rutile, glaucophane, and omphacite. The inclusion mineralogy varies from clinozoisite and glaucophane in the core to omphacite and quartz in the rim, which defines a clockwise prograde metamorphic *P-T* path from blueschist to eclogite facies (Figs. 1a and 1b). In contrast, small garnets contain minor inclusions of quartz, rutile, and omphacite but are free of glaucophane and clinozoisite (Figs. 1c and 1d). Inclusion-free garnets with euhedral shapes are also observed; however, small ragged garnets are absent, indicating that most small garnets are not the relics of large crystals (Figs. 1e and 1f). Most garnets are rimmed by narrow retrograde coronas of sodic amphibole. Compositional zoning patterns of garnets vary with their sizes. Patterns typical of prograde growth zoning were observed in large garnets (~1 mm): Ca shows a continuous decrease in concentration toward rims, whereas Fe is relatively constant across the traverses. Manganese shows a peak in the center, a sharp decrease toward the rim, and a slight increase near the rim, whereas Mg shows a pronounced increase toward the rim (Fig. 3).

Three distinct domains can be defined in the large garnets from the zoning patterns and the abundances of inclusions: (1) an inclusion-poor, Mn-enriched, Ca-enriched, and Mg-depleted core; (2) an inclusion-rich mantle between the core and rim domain; and (3) a Ca-depleted, Mg-enriched, Mn-enriched, and inclusion-free rim (Fig. 1). In contrast, faint compositional zoning can be observed in small garnets, although some crystals lack chemical zonation (Figs. 1a–1f and 3). In both samples, all garnets show similar rim compositions, but core compositions vary with garnet sizes and core MnO contents generally increase with garnet diameters (Fig. 4). However, this relation is obscured for small garnets (<~500 μm).

Crystal-size and spatial distributions of garnets

The size and spatial distributions of garnets in the two eclogites measured by serial grinding are presented in Figure 5 as histograms of crystal sizes together with 3-D cartoon illustrations. There were 584 and 422 garnets centered within 20.4 × 18.6 × 9.8 and 17.5 × 15.4 × 9.8 mm volumes, respectively (Figs. 5g and 5h). The chi-square (χ^2) test for the four quarters of the TH12 volume, which yielded a value of 0.77 [$\chi^2_{0.05(3)} = 7.815$ at the 95% confidence interval and 3 degrees of freedom], confirmed the homogeneity of garnet distribution at this scale (Figs. 5a–5d). The mean distances for the two volumes, averages of the distance from each of the garnet crystals to their nearest neighbor, were

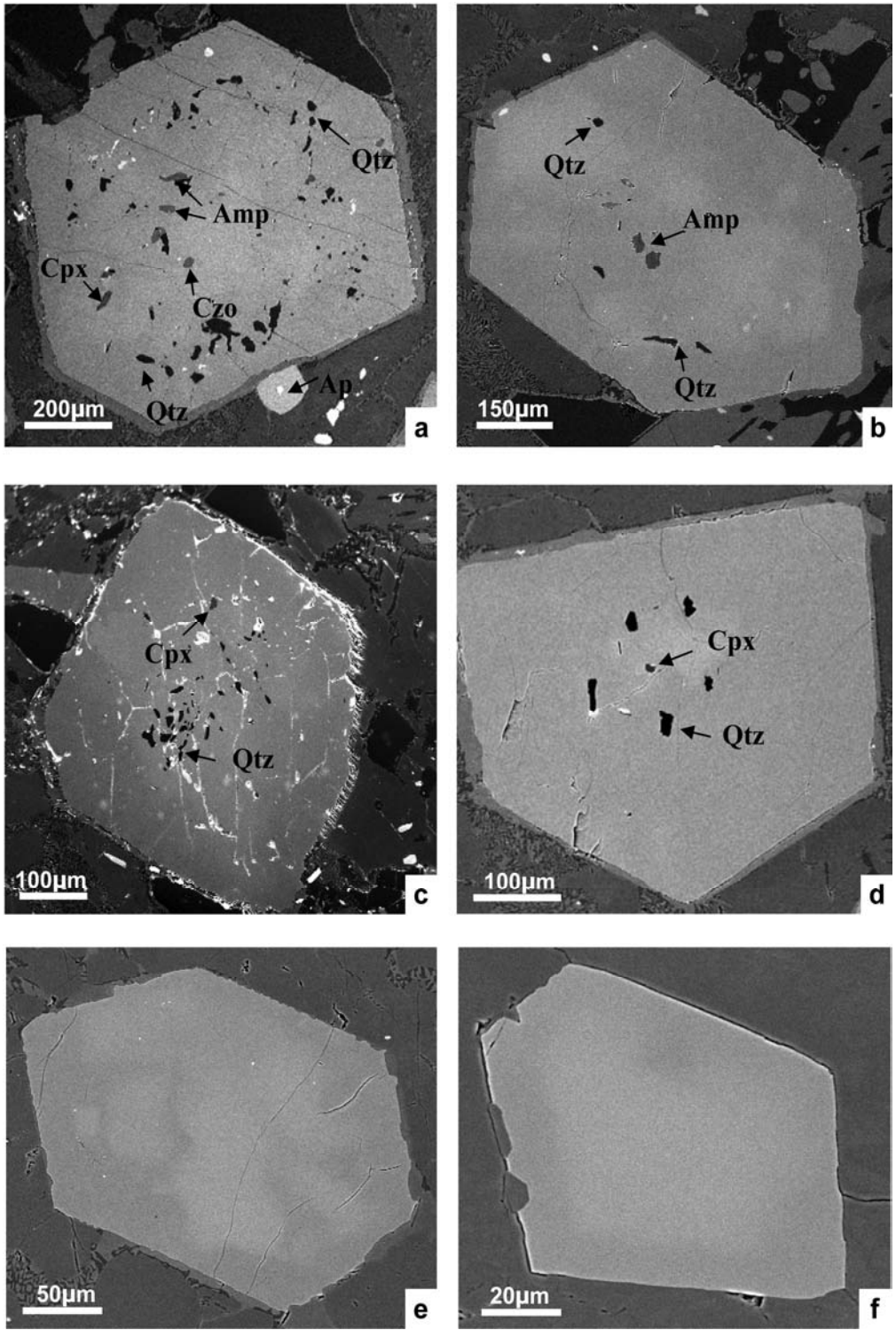

FIGURE 1. Back-scattered electron images of representative garnets with distributed inclusions. Grt = garnet; Qtz = quartz; Czo = clinozoisite; Ap = apatite; Amp = amphibole; Cpx = clinopyroxene.

found to be 1.05 and 1.07 mm, consistent with the theoretic randomness values of 1.02 and 1.03 mm (Chandrasekhar 1943), respectively, indicating the random spatial distribution of garnets. Both samples show similar considerably positively skewed (Figs. 5e and 5f) and quasi-lognormal CSDs with slight shifts to the right of the theoretic lognormal curves (Fig. 6).

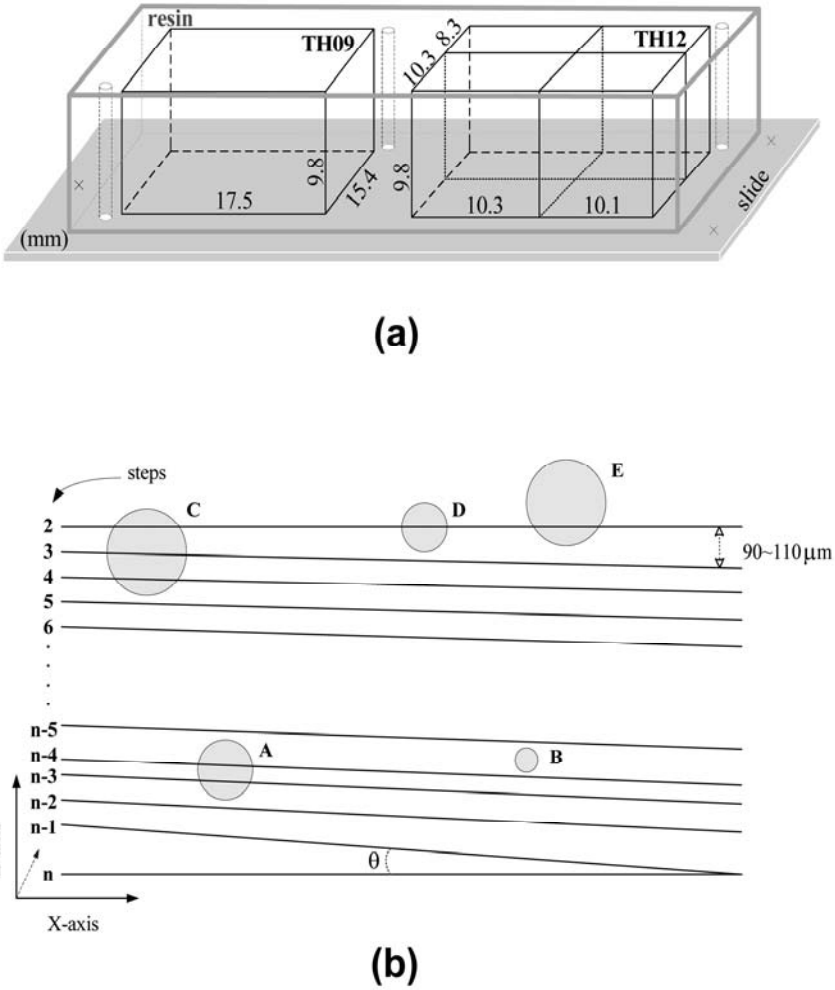

FIGURE 2. (**a**) Cartoon of the sample preparation strategy prior to serial grinding. Cross marks were used to initialize the stage and for coordinate transformation. (**b**) Procedure for determining the size of garnet crystals encountered in various locations (A–E). The angle θ was divided by $n - 2$ to give a tilt calibration for each step during grinding.

DISCUSSION

Chemical zoning in metamorphic garnet has long been regarded as a record of the metamorphic processes governing garnet crystallization (e.g., Kohn 2003). In addition, textural analysis may potentially provide insight into the overlapping generations of garnet growth, including original nucleation and later growth environments. Therefore, the size and spatial distributions, in conjunction with the compositional analyses, can be used to reconstruct the nucleation and growth of the metamorphic garnets in Dabie eclogites. We argue that the apparent pseudo-lognormal distributions of garnets could be attributed to different nucleation and growth rates within three distinct formation episodes based on the CSD data, chemical zoning, and the mineral inclusions.

Nucleation and growth model

The barrier to nucleation is attributed to the interfacial energy according to classical nucleation theory. The overall nucleation rate relies on thermal overstepping and interfacial energy as well as the chemical free energy change related to the phase transformation (e.g., Carlson 1999), and the nucleation still remains the least well-characterized processes for porphyroblast crystallization (Hirsh and Carlson 2006). Manganese strongly partitions into garnet, as recognized in previous studies (e.g., Hollister 1966). Numerous studies suggest that it is reasonable to utilize Mn zoning as a proxy for garnet nucleation and growth during thermal evolution based on the correlation between garnet sizes and core MnO compositions (e.g., Kretz 1974, 1993; Cashman and Ferry 1988; Carlson 1989; Spear 1993), although coalescence of multiple nuclei is responsible for garnets in certain rocks (Daniel and Spear 1998).

By the use of serial grinding, sections were obtained approximately across the centers of several garnets. The generally positive correlation between core MnO contents and garnets diameters (Fig. 4a) is consistent with phase-equilibria predictions (Spear 1993) and numerous observations in the literature. This correlation indicates that garnets with high-Mn cores nucleated first and preserve a longer record of the metamorphism as compared to garnets characterized by low-Mn core compositions that most likely crystallized later in the metamorphic history.

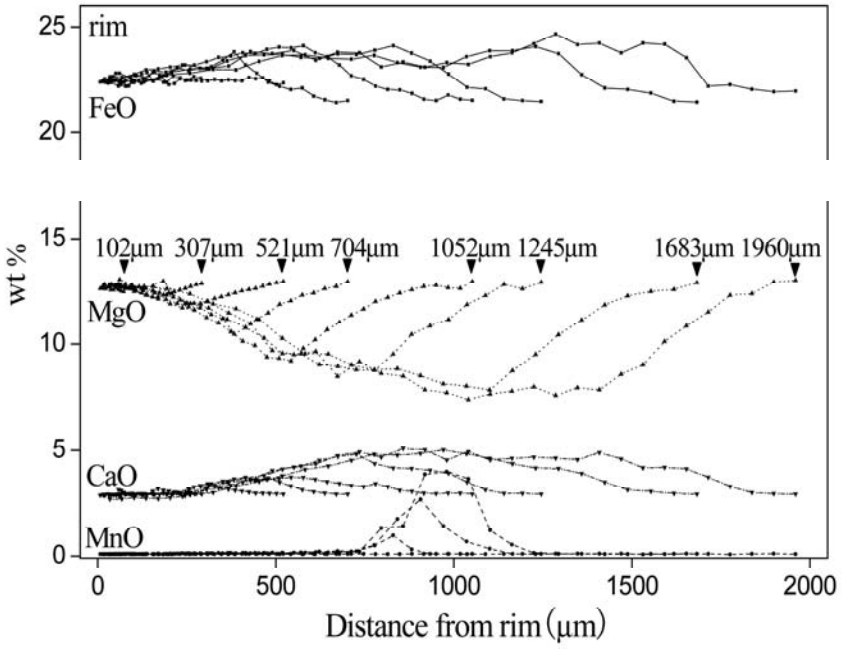

FIGURE 3. Compositional zoning profiles plotted against distance from the rim for various sized garnets.

The various sizes with similar core MnO compositions could be attributed to either varying growth rates in the earlier episode or/and various numbers of nuclei pre-incorporated within a single garnet (Daniel and Spear 1998). The latter is difficult to rule out solely based on the smooth MnO zoning patterns and lack of the isolated high-MnO areas within a single garnet because diffusional re-equilibration tends to eliminate evidence of the early nuclei at the peak metamorphic temperatures of 640–670 °C for the studied eclogites (Florence and Spear 1991). Yet, identical crystallographic orientations for single garnet crystals (Cheng et al. 2007) suggest that (1) varying growth rates were likely the dominant mechanism responsible for variation of garnet sizes with similar core MnO values; (2) nucleation was continuous; and (3) the core compositions can be used as an index to decipher the relative timing of nucleation of each garnet.

Rim compositions for garnets of differing sizes approximately overlap when their rims are aligned (Fig. 3), indicating an overall constant radius growth mechanism controlled by surface reaction (Kretz 1974). Nevertheless, the notable absence of high-MnO core compositions for small garnets (<~500 μm) and the absence of a correlation between diameter and MnO core compositions for small garnets (Fig. 4) indicate a nucleation and growth history distinct from large ones. In support of this interpretation, we note that the mineralogy of inclusions in garnet varies with crystal size: large garnets (≥~1.0 mm) generally contain all the index phases along the prograde path; middle-sized garnets mostly contain quartz inclusions, and products of the former blueschist-facies index minerals breakdown, such as clinozoisite and amphibole. Most small garnets (≤~500 μm), on the other hand, have inclusions similar to those found in the outer rims of large garnets (Fig. 7). We conclude that most small garnets and the outer rims of the large garnets were likely formed in a distinct fluid-enhanced overgrowth episode rather than a continuation of the earlier growth stage of the large garnet cores (Cheng et al.

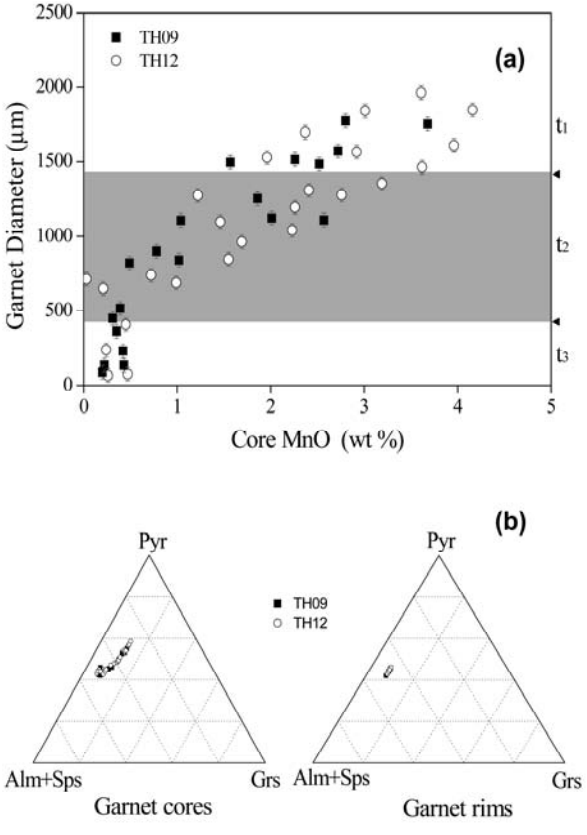

FIGURE 4. (**a**) Garnet diameter plotted as function of core MnO concentration. Error bar is 2σ. Three episodes t_1, t_2, t_3 are indicated. (**b**) Composition diagrams for garnet cores and rims. Alm = almandine; Pyr = pyrope; Grs = grossular; Sps = spessartine.

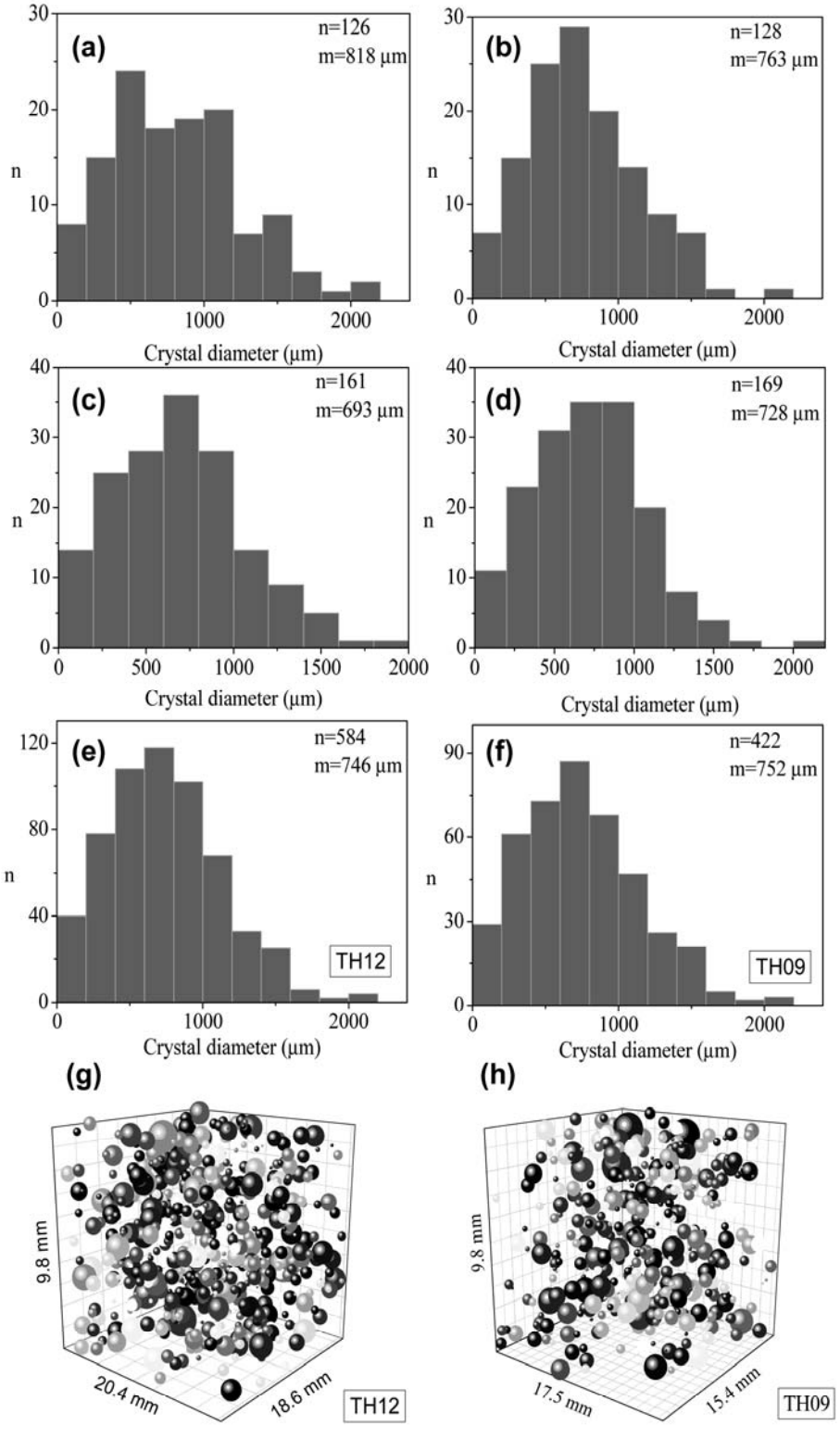

FIGURE 5. Histograms of measured crystal sizes of four quarters (**a**–**d**) of TH12 and TH09. The four quarters of TH12 are also combined into one histogram for clarity (**e**). Numbers of data (*n*) and mean values (*m*) are represented in each histogram. The 3D model of spatial distribution of garnet crystals in both samples is also illustrated (**g**,**h**), in which garnets are simplified to equivalent spheres in scale with true crystals and randomly rendered in various grayscales for clarity.

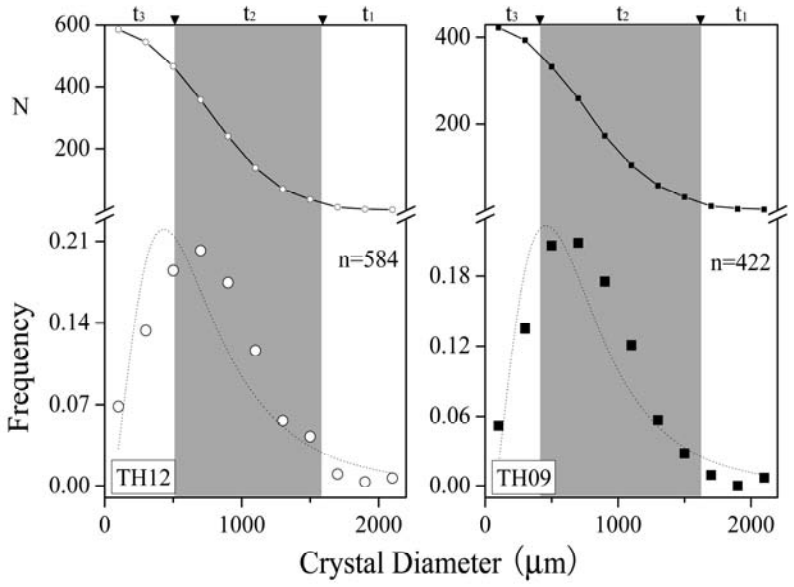

FIGURE 6. Crystal-size (scatter points) and reverse cumulative distribution (solid line with symbols). Dotted lines are theoretical lognormal curves fitted to these data. Three episodes, t_1, t_2, t_3, and number of the data are also indicated.

2007). Therefore, size-independent constant radius growth rate is here preferred to interpret the crystal-size data.

The age of UHP metamorphism in the Dabie orogen is well constrained to be Middle-Late Triassic. Nevertheless, UHP recrystallization may have spanned from as early as ~245 to ~220 Ma (e.g., Hacker et al. 1998, 2000; Li et al. 2000). Sm-Nd mineral isochron ages of ~226 Ma and U-Pb zircon ages of ~224 Ma were interpreted as the timing of peak UHP metamorphism in Central Dabie (e.g., Li et al. 2000; Zheng et al. 2007). On the other hand, the ~210 Ma ages were suggested for regional amphibolite-facies overprinting resulting from pervasively retrograde fluid infiltration (e.g., Ayers et al. 2002; Liu et al. 2006). Intervals for the garnet growth-related subduction and exhumation hereby are estimated to be about 20 and 15 Ma, respectively. Thus, the radial distance from the center of the largest garnet is a time index and a cumulative curve for the reverse histogram thus can provide insight into nucleation rate (Fig. 6). First, at the onset of time interval t_1, temperature started to increase with subduction, the free energy for the formation of garnet increased significantly, reducing the nucleation energy, which resulted in an increasing nucleation rate, and relatively few largest garnets emerged. Second, the rocks experienced a slower increase of temperature for a relatively long residence t_2; during this interval, the system reached a near steady-state condition, resulting in a relatively constant nucleation rate producing middle-size garnets. Finally, during the time interval t_3, temperature was constant or declined, inhibiting favorable nucleation sites due to the lack of thermal overstepping, decreasing the nucleation rate (Fig. 6). The effect of fluid on nucleation during t_3 is unclear. A similar model for garnets from highly deformed gneiss was proposed by Kretz (2006). Estimation of the absolute garnet growth rate is hindered by the restricted radiogenic dating results corresponding to specific garnet growth stages. Using the largest garnets (~2.0 mm), given that the outermost rim was formed during the t_3 and the inner part was formed during t_1 and t_2, growth rates of 0.25 and 0.13 μm/Ma for prograde growth and overgrowth, respectively, can be approximated.

Nevertheless, given that the strategy of separating bulk garnets is applied in geochronological studies, and that inclusion-rich cores may be selectively discarded, small garnets and the large garnet rims that grew during t_3 may dominate resulting ages. Garnet geochronology by methods such as garnet Sm-Nd system could, therefore, yield the latest overgrowth age rather than the peak metamorphic age or an average age of the whole UHP metamorphic process. Likewise, given micro-sampling and highly sensitive mass spectrometric facilities, the growth rates of rocks can be constrained from the difference between the overgrowth rim and bulk ages of a garnet similar to cooling rates (Ganguly et al. 1998).

Crystal-size distribution analysis

Eberl et al. (1998) predicted three basic CSD shapes derived from various crystal growth mechanisms, i.e., the asymptotic distribution, the lognormal distribution, and Lifshitz-Slyozov-Wagner (LSW) distribution (Lifshitz and Slyozov 1961; Wagner 1961). Minerals in numerous metamorphic rocks show lognormal or pseudo-lognormal CSD shapes (e.g., Cashman and Ferry 1988; Azpiroz and Fernandez 2003; Carlson 1999; Kaneko et al. 2005), which are attributed to kinetic controls on nucleation and growth. The size distributions of garnet in Dabie metamorphic eclogites are also found in pseudo-lognormal shapes with a slight rightward shift off theoretical lognormal curves (Fig. 6). In addition to Ostwald ripening, two distinct rate-limiting growth models have been proposed for apparent pseudo-lognormal distributions: thermally accelerated, diffusion-controlled (TADC) nucleation and growth (Carlson et al. 1995; Carlson 1999); and size-dependent (proportionate) growth according to the law of proportionate effect (LPE) (Eberl et al. 1998), which is argued

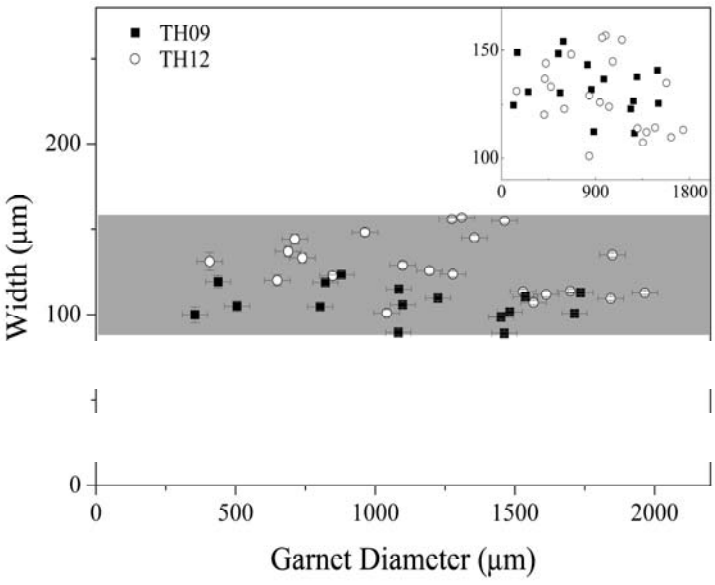

FIGURE 7. Width of inclusion-free rim plotted as function of garnet diameter shows restricted variation of widths uncorrelated with garnet diameters. Error bar is 2σ. The inset plot shows no correlation between the overgrown garnet width and the garnet diameter prior to overgrowth, as determined by subtracting the overgrown width from the overall diameter.

to be related to the supply of reactants to the crystal surface (Kile and Eberl 2003).

Ostwald ripening

Ostwald ripening (coarsening) is the phenomenon by which smaller particles are essentially consumed by larger particles during the growth process due to the Gibbs-Thomson effect. So far the assumptions in Lifshitz-Slyozov-Wagner theory have led to frequent disagreements between theoretical and experimental results (Cushing et al. 2004, and references therein). The Ostwald ripening was introduced to explain the departure from linearity for garnets in metamorphic pelites by Cashman and Ferry (1988) in crystal-size distribution analysis, which was also advocated by Miyazaki (1991). However, subsequent studies have discredited this hypothesis and argued that enlargement of crystals via Ostwald ripening is unlikely to occur in multiphase metamorphic rock systems (Carlson 1999; Kretz 2006). In our samples, the right-shift of the CSDs off the theoretical lognormal curves may apparently indicate Ostwald ripening (Fig. 6); if so, rounded edges on small garnet crystals would be expected given that coarsening of large garnets would occur at the expense of smaller grains, and this is not observed (Fig. 1). Furthermore, the restricted width (125 ± 30 μm) of the overgrown outer rims, regardless of garnet size, cannot be explained by coarsening (Fig. 7), which increases average size with constant volume fraction. Therefore, the right-shift of the theoretical lognormal curves is more simply interpreted as varying nucleation and growth rates.

The TADC model

Carlson (1999) showed that the typical lognormal CSDs in metamorphic rocks could be reproduced through a thermally accelerated, diffusion-controlled (TADC) nucleation and growth mechanism instead of Ostwald ripening. According to the TADC model, the pseudo-lognormal distribution is attributed to an increasing heating rate followed by a decreasing heating rate, in which the former produced a positively skewed lognormal distribution and the latter adjusted the curve toward a near-symmetric distribution resulting in a pseudo-lognormal curve as a whole. However, the predicted stranded diffusion gradients, potentially expected as compositional spikes within garnets (Carlson et al. 1995; Carlson 1989), are not observed in the Dabie samples (Fig. 3). Moreover, the bell-shaped MnO and heavy rare-earth-element (HREEs) compositional profiles (Cheng et al. in prep.) can readily be modeled using Rayleigh fractionation (Hollister 1966). Although the TADC nucleation and growth cannot be completely ruled out as a mechanism for specific garnet growth episodes as the TADC model can account for the overall CSDs of garnets in the samples, a surface-kinetics controlled growth mechanism with constant radius growth rate is favored.

The proportionate growth model

In an attempt to explore the CSDs, Eberl et al. (1998) provided an alternative method based on a size-dependent (proportionate) growth law, although its thermodynamics and kinetics remain to be explored. This method implies that all of the crystals could have nucleated at the same time, with those in the right tails of the CSDs having grown larger as a result of size-dependent growth and growth dispersion (Eberl et al. 1998). However, the linear correlation between the garnet sizes and the core MnO compositions disfavor this model but support the interpretation that the largest garnet is the oldest one, which is consistent with the size-independent growth mechanism as a whole. Furthermore, a linear and a hyperbolic correlation between overgrowth width and crystal diameter prior to overgrowth are expected for the proportionate growth ($dr/dt \propto r$) and diffusion-controlled ($dr/dt \propto 1/r$) growth, respectively, where r is garnet diameter and t is time. Yet, neither correlation could be observed (Fig. 7). Thus, the uniform width of the overgrown outer rims, regardless of garnet sizes, cannot be explained by either the proportionate growth or diffusion-control mechanism alone. In addition, Ostwald ripening has to be taken into account to simulate the CSDs of these samples by the proportionate growth mechanism (Fig. 6), which is suspicious as mentioned above. A possible explanation for why

the size-dependent growth did not prevail is (1) initial growth conditions provided restricted growth rate dispersions so as to produce limited differences in initial crystal sizes during t_1; thus, (2) size-dependent growth cannot occur (McCabe's Law is valid; McCabe and Stevens 1951), possibly due to increasing nucleation rate during the second interval t_2. Therefore, the CSDs record nucleation and growth history instead of merely the products of growth mechanism in these samples.

Concluding remarks

Understanding chemical zoning patterns and growth mechanisms in garnets are the key for deciphering garnet-related Sm-Nd and Lu-Hf geochronological studies (e.g., Lapen et al. 2003). Combined chemical analysis and CSD analysis of metamorphic rocks can therefore not only provide opportunities for insight into the genesis of the garnets but also provide new clues to the interpretation of geochronological studies. Our data indicate three distinct garnet nucleation and growth processes in UHP metamorphic eclogites, which should result in different garnet regions with various Nd/Sm and Lu/Hf ratios. Given that the strategy of separating bulk garnets is applied in geochronological studies, various Sm-Nd and Lu-Hf dating results could be expected to give a mixture timing of the overall nucleation and growth processes. Nevertheless, providing mineral separation bias occurred, i.e., the inclusion-free garnet portions tend to be picked during mineral separating procedure; an apparently younger age skewing toward the last growth episode is predictable. Microsampling technology is therefore advocated to retrieve the exact garnet growth history (Ganguly et al. 1998).

Acknowledgments

We thank R.L. King for reading an earlier draft and correcting the English. Z.Y. Zhou is thanked for providing garnet standards. We also thank Y. Chang for his help in sample preparation. The manuscript benefited from the constructive and thorough reviews of Y. Xiao and R. Jonckheere. This study was funded by grants from the Natural Science Foundation of China (40403007, 40572075) and from the "Center of Excellence for 21st Century in Japan" program (to E. Nakamura).

References cited

Ames, L., Tilton, G.R., and Zhou, G. (1993) Timing of collision of the Sino-Korean and Yangtze Cratons. U-Pb zircon dating of coesite-bearing eclogites. Geology, 21, 339–342.

Armienti, P. and Tarquini, S. (2002) Power law olivine crystal size distributions in lithospheric mantle xenoliths. Lithos, 65, 273–285.

Armienti, P., Pareschi, M.T., Innocenti, F., and Pompilio, M. (1994) Effects of magma storage and ascent on the kinetics of crystal growth. The case of 1991–93 Mt. Etna eruption. Contributions to Mineralogy and Petrology, 115, 402–414.

Ayers, J.C., Dunkle, S., Gao, S., and Miller, C.E. (2002) Constraints on timing of peak and retrograde metamorphism in the Dabie Shan ultrahigh-pressure metamorphic belt, eastcentral China, using U-Th-Pb dating of zircon and monazite. Chemical Geology, 186, 315–331.

Azpiroza, M.D. and Fernández, C. (2003) Characterization of tectono-metamorphic events using crystal size distribution (CSD) diagrams. A case study from the Acebuches metabasites (SW Spain). Journal of Structural Geology, 25, 935–947.

Browne, B.L., Browne, J.C., Patino, L.C., Vogel, T.A., Uto, K., and Hooshizumi, H. (2006) Magma mingling as indicated by texture and Sr/Ba ratios of plagioclase phenocrysts from Unzen volcano, SW Japan. Journal of Volcanology and Geothermal Research, 154, 103–116.

Bryon, D.N., Atherton, M.P., and Hunter, R.H. (1995) The interpretation of granitic textures from serial thin sectioning, image analysis and three-dimensional reconstruction. Mineralogical Magazine, 59, 203–211.

Carlson, W.D. (1989) The significance of intergranular diffusion to the mechanisms and kinetics of porphyroblast crystallization. Contributions to Mineralogy and Petrology, 103, 1–24.

——— (1999) The case against Ostwald ripening of porphyroblasts. Canadian Mineralogist, 37, 403–413.

Carlson, W.D., Denison, C., and Ketcham, R.A. (1995) Controls on the nucleation and growth of porphyroblasts: Kinetics from natural textures and numerical models. Geological Journal, 30, 207–225.

Carswell, D., O'Brien, P., and Wilson, R. (1997) Thermobarometry of phengite-bearing eclogites in the Dabie mountains of central China. Journal of Metamorphic Geology, 15, 239–252.

Cashman, K.V. and Ferry, J.M. (1988) Crystal size distribution (CSD) in rocks and the kinetics and dynamics of crystallization. III. Metamorphic crystallization. Contributions to Mineralogy and Petrology, 99, 401–415.

Cashman, K.V. and Marsh, B.D. (1988) Crystal size distribution (CSD) in rocks and the kinetics and dynamics of crystallization. II. Makaopuhi lava lake. Contributions to Mineralogy and Petrology, 99, 292–305.

Castelli, D., Rolfo, F., and Compagnoni, R. (1998) Metamorphic veins with kyanite, zoisite and quartz in the Zhu-Jia-Chong eclogite, Dabie Shan, China. Island Arc, 7, 159–173.

Chandrasekhar, S. (1943) Stochastic problems in physics and astronomy. Reviews of Modern Physics, 15, 1–89.

Cheng, H., Nakamura, E., Kobayashi, K., and Zhou Z.Y. (2007) Origin of atoll garnets in eclogites and implications for the redistribution of trace elements during slab exhumation in a continental subduction zone. American Mineralogist, 92, 1119–1129.

Cooper, M.R. and. Hunter, R.H. (1995) Precision serial lapping, imaging and three-dimensional reconstruction of minus-cement and post-cementation intergranular pore-systems in the Penrith Sandstone of north-western England. Mineralogical Magazine, 59, 213–220.

Cushing, B.L., Kolesnichenko, V.L., and O'Connor, C.J. (2004) Recent advances in the liquid-phase syntheses of inorganic nanoparticles. Chemical Reviews, 104, 3893–3946.

Daniel, C.G. and Spear, F.S. (1998) Three-dimensional patterns of garnet nucleation and growth. Geology, 26, 503–506.

Denison, C. and Carlson, W.D. (1997) Three-dimensional quantitative textural analysis of metamorphic rocks using high resolution computed X-ray tomography. Part II: Application to natural samples. Journal of Metamorphic Geology, 15, 45–57.

Eberl, D.D., Drits, V.A., and Srodon, J. (1998) Deducing growth mechanisms for minerals from the shapes of crystal size distributions. American Journal of Science, 298, 499–533.

Eberl, D.D., Kile, D.E., and Drits, V.A. (2002) On geological interpretations of crystal size distributions: Constant vs. proportionate growth. American Mineralogist, 87, 1235–1241.

Eide, L., McWilliams, M., and Liou, J.G. (1994) $^{40}Ar/^{39}Ar$ ages constrain exhumation of high and very high pressure metamorphic rocks in eastern central China. Geology, 22, 601–604.

Florence, F.P. and Spear, F.S. (1991) Effects of diffusional modification of garnet growth zoning on *P-T* path calculations. Contributions to Mineralogy and Petrology, 107, 487–500.

Ganguly, J., Tirone, M., and Hervig, R. (1998) Diffusion kinetics of samarium and neodymium in garnet, and a method of determining cooling rates of rocks. Science, 281, 805–807.

Gualda, G.A.R. and Rivers, M. (2006) Quantitative 3D petrography using X-ray tomography: Application to Bishop Tuff pumice clasts. Journal of Volcanology and Geothermal Research, 154, 48–62.

Hacker, B.R., Ratschbacher, L., Webb, L., Ireland, T., Walker, D., and Dong, S. (1998) U/Pb zircon ages constrain the architecture of the ultrahigh-pressure Qinling-Dabie Orogen, China. Earth and Planetary Science Letters, 161, 215–230.

Hacker, B.R., Webb, L.E., Ireland, T.R., Calvert, A., Dong, S., Wenk, H.R., and Chateigner, D. (2000) Exhumation of ultrahigh-pressure continental crust in east-central China: Late Triassic-Early Jurassic tectonic unroofing. Journal of Geophysical Research, 105, 13339–13364.

Higgins, M.D. (1994) Determination of crystal morphology and size from bulk measurements on thin sections: Numerical modeling. American Mineralogist, 79, 113–119.

——— (1996) Magma dynamics beneath Kameni Volcano, Greece, as revealed by crystal size and shape measurements. Journal of Volcanology and Geothermal Research, 70, 37–48.

——— (1998) Origin of anorthosite by textural coarsening: quantitative measurements of a natural sequence of textural development. Journal of Petrology, 39, 1307–1325.

——— (2002) A crystal size-distribution study of the Kiglapait layered mafic intrusion, Labrador, Canada: evidence for textural coarsening. Contributions to Mineralogy and Petrology, 144, 314–330.

Hirsh, D.M. and Carlson, W.D. (2006) Variations in rates of nucleation and growth of biotite porphyroblasts. Journal of Metamorphic Geology, 24, 763–777.

Hollister, L.S. (1966) Garnet zoning: An interpretation based on the Rayleigh fractionation model. Science, 154, 1647–1651.

Kaneko, Y., Tsunogae, T., and Miyano, T. (2005) Crystal-size distributions of garnets in metapelites from the northeastern Bushveld contact aureole, South

Africa. American Mineralogist, 90, 1422–1433.
Kile, D.E. and Eberl, E.E. (2003) On the origin of size-dependent and size-independent crystal growth: Influence of advection and diffusion. American Mineralogist, 88, 1514–1521.
Kinman, W.S. and Neal, C.R. (2006) Magma evolution revealed by anorthite-rich plagioclase cumulate xenoliths from the Ontong Java Plateau: insights into LIP magma dynamics and melt evolution. Journal of Volcanology and Geothermal Research, 154, 131–157.
Kohn, M.J. (2003) Geochemical zoning in metamorphic minerals. In R. L. Rudnick Eds., Treatise on Geochemistry, The Crust, 3, p. 229–261, Geological Society Publishing House, U.K.
Kretz, R. (1974) Some models for the rate of crystallization of garnet in metamorphic rocks. Lithos, 7, 123–131.
——— (1993) A garnet population in Yellowknife schist, Canada. Journal of Metamorphic Geology, 11, 101–120.
——— (2006) Shape, size, spatial distribution and composition of garnet crystals in highly deformed gneiss of the Otter Lake area, Québec, and a model for garnet crystallization. Journal of Metamorphic Geology, 24, 431–449.
Lapen, T.J., Johnson, C.M., Baumgartner, L.P., Mahlen, N.J., Beard, B.L., and Amato, J.M. (2003) Burial rates during prograde metamorphism of an ultra-high-pressure terrane: An example from Lago di Cignana, western Alps, Italy. Earth and Planetary Science Letters, 215, 57–72.
Li, S., Jagoutz, E., Chen, Y., and Li, Q. (2000) Sm-Nd and Rb-Sr isotopic chronology and cooling history of ultrahigh pressure metamorphic rocks and their country rocks at Shuanghe in the Dabie Mountains, Central China. Geochimica et Cosmochimica Acta, 64, 1077–1093.
Li, X., Zheng, Y.F., Wu, Y., Chen, F., Gong, B., and Li, Y. (2004) Low-*T* eclogite in the Dabie terrane of China: Petrological and isotopic constraints on fluid activity and radiometric dating. Contributions to Mineralogy and Petrology, 148, 443–470.
Lifshitz, I.M. and Slyozov, V.V. (1961) The kinetics of precipitation from supersaturated solid solutions. Journal of Physical Chemistry Solids, 19, 35–50.
Liu, D.Y., Jian, P., Kröner, A., and Xu, S.T. (2006) Dating of prograde metamorphic events deciphered from episodic zircon growth in rocks of the Dabie-Sulu UHP complex, China. Earth and Planetary Science Letters, 250, 650–666.
Marsh, B.D. (1988) Crystal size distribution (CSD) in rocks and the kinetics and dynamics of crystallization: I. Theory. Contributions to Mineralogy and Petrology, 99, 277–291.
Martin, V.M., Holness, M.B., and Pyle, D.M. (2006) Textural analysis of magmatic enclaves from the Kameni Islands, Santorini, Greece. Journal of Volcanology and Geothermal Research, 154, 89–102.
McCabe, W.L. and Stevens, R.P. (1951) Rate of growth of crystals in aqueous solutions. Chemical Engineering Progress, 47, 168–174.
Miyazaki, K. (1991) Ostwald ripening of garnet in high *P/T* metamorphic rocks. Contributions to Mineralogy and Petrology, 108, 118–128.
Mock, A. and Jerram, D.A. (2005) Crystal size distributions (CSD) in three dimensions: Insights from the 3D reconstruction of a highly porphyritic rhyolite. Journal of Petrology, 46, 1525–1541.
Okay, A. (1993) Petrology of a diamond and coesite-bearing metamorphic terrain: Dabie Shan, China. European Journal of Mineralogy, 5, 659–675.
Peterson, T.D. (1990) Petrology and genesis of natrocarbonatite. Contributions to Mineralogy and Petrology, 105, 143–155.
Rowe, T., Kappelman, J., Carlson, W.D., Ketcham, R.A., and Denison, C. (1997) High-resolution computed tomography: A breakthrough technology for earth scientist. Geotimes, 42, 23−27.
Rowley, D.B., Xue, F., and Tucker, R.D. (1997) Ages of ultra–high pressure metamorphic and protolith orthogneisses from the eastern Dabie Shan: U/Pb zircon geochronology. Earth and Planetary Science Letters, 151, 191–203.
Shi, Y. and Wang, Q. (2006) Variation in peak *P-T* conditions across the upper contact of the UHP terrane, Dabieshan, China: gradational or abrupt? Journal of Metamorphic Geology, 24, 803–822.
Spear, F.S. (1993) Metamorphic phase equilibria and pressure-temperature-time paths, 1, 799 p. Monograph, Mineralogical Society of America, Chantilly, Virginia.
Wagner, C. (1961) Theorie der alterung von niederschlagen durch umlosen (Ostwald Reifung). Zeitschrift feur Elektrochemie, 65, 581–591.
Wang, X. and Liou, J.G. (1991) Regional ultrahigh-pressure coesite-bearing eclogitic terrane in central China: Evidence from country rocks, gneiss, marble, and metapelite. Geology, 19, 933–936.
Wilhelm, S. and Wörner, G. (1996) Crystal size distribution in Jurassic Ferrar flows and sills (Victoria Land, Antartica): Evidence for processes of cooling, nucleation and crystallisation. Contributions to Mineralogy and Petrology, 125, 1–15.
Zheng, Y.F., Gao T.S., Wu, Y.B., Gong, B., and Liu, X.M. (2007) Fluid flow during exhumation of deeply subducted continental crust: zircon U-Pb age and O-isotope studies of a quartz vein within ultrahigh-pressure eclogite. Journal of Metamorphic Geology, 25, 267–283.

Manuscript received January 4, 2007
Manuscript accepted September 11, 2007
Manuscript handled by Raymond Jonckheere